UNSOLVED PROBLEMS IN PLANETARY RING DYNAMICS

NICOLE BORDERIES, PETER GOLDREICH
California Institute of Technology

and

SCOTT TREMAINE
Massachusetts Institute of Technology

We discuss a number of unsolved problems in planetary ring dynamics and offer some thoughts concerning their solution. The discussion is specialized to the rings of Saturn because they are the best studied observationally. The depth of treatment varies from problem to problem and reflects both limitations in our understanding and the relative importance which we attach to different topics. We make no attempt to present material in a tutorial style. We deal with phenomena that are microscopic and macroscopic on the scale set by the resolution of the Voyager cameras. We relate the physics of particle collisions (Sec. I) to the local velocity dispersion (Sec. II) and the particle size distribution (Sec. III). We discuss mechanisms which structure the rings (Sec. IV) and affect the orbital evolution of satellites which interact with them (Sec. V).

I. PARTICLE COLLISIONS

A. Mechanical Properties of the Particles

The mechanical properties are largely characterized by the elastic modulus E and the yield modulus σ_Y. These moduli are properly described by tensors but for our rough calculations their scalar magnitudes suffice.

The elastic modulus is the ratio of the stress to the strain. It has the dimensions of force per unit area or energy per unit volume. The latter reflects its close relation to the molecular bond energy per unit volume. For common materials the molecular bond energy is of order one electron volt and the molecular size is of order one angstrom. It follows that the elastic modulus is $\sim 10^{12}$ dyne cm^{-2}. For ice its value is smaller, $\sim 10^{11}$ dyne cm^{-2} (Hobbs 1974), because the hydrogen bond is weak.

The yield modulus is the limiting stress beyond which ice fractures. Its value decreases with increasing temperature, especially near to the melting temperature. We have been able to find only a single reference to measurements of the yield stress of ice at temperatures comparable to those in Saturn's rings. These experiments obtained values $\sim 3 \times 10^8$ dyne cm^{-2} at $T = 77$ K for the compressive yield stress (Parameswaran and Jones 1975).

For future discussion we adopt the values $E = 10^{11}$ dyne cm^{-2} and $\sigma_Y = 10^8$ dyne cm^{-2}. We choose a smaller value for σ_Y than quoted above because collisions generate comparable compressive, shear, and tensile stresses, and the compressive yield modulus of ice is larger than either the shear or tensile yield modulus. We also use $\mu = 0.36$ for the Poisson ratio. It must be kept in mind that the numerical values we are adopting refer to solid and chemically pure ice and thus may not directly apply to the properties of the particles in Saturn's rings.

B. Dynamics of Collisions

The imperfectly elastic nature of the impacts is described by the coefficient of restitution ϵ, the factor by which the relative normal velocity is reduced following a collision. We need to relate ϵ to E and σ_Y.

The Hertz (1881) law of contact describes purely elastic, low-velocity, impacts. When applied to the collision of two identical smooth spheres of radius R, density ρ, and relative impact velocity v, it gives the following expressions for the maximum radius of the area of contact a and the maximum stress σ_M:

$$a/R \simeq (\rho v^2/E)^{\frac{1}{5}}, \tag{1}$$

$$\sigma_M/E \simeq 0.7\,(\rho v^2/E)^{\frac{1}{5}}. \tag{2}$$

From the latter relation we find that the yield stress of ice is reached at an impact velocity of 0.03 cm s^{-1}.

For higher velocity impacts, account must be taken of brittle fracture near the area of contact. The best theory that we have been able to find to apply in this case is due to Andrews (1930). It is designed to treat impacts of soft metals and includes plastic as well as elastic deformation. It is far from rigorous even for its intended application and we shall apply it where failure occurs by brittle fracture rather than by plastic flow. Thus the conclusions we derive from Andrews' theory are to be taken with caution.

Andrews views an impact as taking place in the three stages illustrated in Fig. 1. There is an initial elastic compression which lasts until the critical stress is reached. It is followed by continued compression during which there is an inner circular plastic zone surrounded by an elastic annulus. The stress in the plastic zone is set equal to σ_Y. The restitution which finishes the process is incomplete leaving the sphere permanently flattened. Andrews' theory predicts $\epsilon = 1$ for $v/v^* \leq 1$ and

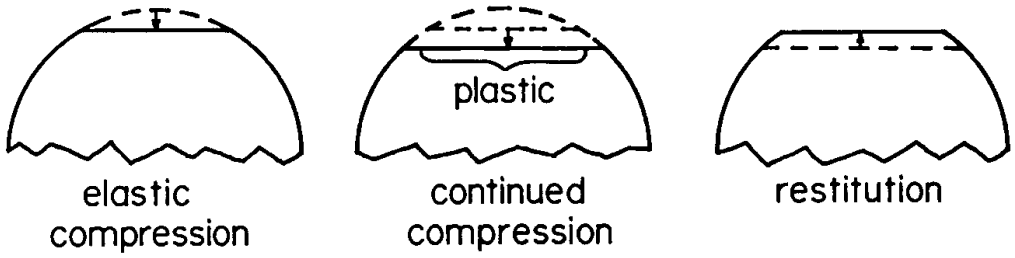

Fig. 1. Three stages of impact in Andrews' theory.

$$\epsilon = \left\{ \frac{-2}{3}\left(\frac{v^*}{v}\right)^2 + \left[\frac{10}{3}\left(\frac{v^*}{v}\right)^2 - \frac{5}{9}\left(\frac{v^*}{v}\right)^4 \right]^{\frac{1}{2}} \right\}^{\frac{1}{2}} \tag{3}$$

for $v/v^* \geq 1$ where

$$v^* = \frac{\pi^2 (1-\mu^2)^2 \sigma_Y^{\frac{5}{2}}}{10^{\frac{1}{2}} E^2 \rho^{\frac{1}{2}}} . \tag{4}$$

For ice, Eq. (4) gives $v^* \sim 0.03$ cm s^{-1}. Fig. 2 shows ϵ as a function of v/v^*. It will be interesting to compare this theoretical prediction with measurements of ϵ (v), for example in the experiments with ice now in progress by Lin and colleagues (see chapter by Stewart et al.).

Collisions between actual ring particles may differ considerably from those considered here. The particles are not of a single size and their surfaces are probably rough. The radii of curvature on a rough surface are smaller than the particle radius so the stress generated in the collision of rough particles is greater than that generated in a similar impact of smooth particles. Consequently, surface roughness lowers the coefficient of restitution (see chapter by Weidenschilling et al.).

II. VELOCITY DISPERSION

The velocity dispersion in a planetary ring depends upon the mechanical properties of the ring particles as expressed through the variation of the coefficient of restitution with impact velocity.

A. Unperturbed Disks

There is a relation between the equilibrium coefficient of restitution and the optical depth τ in a Keplerian disk (Goldreich and Tremaine 1978*a*). This relation depends upon the shape and size distribution of the particles. The function ϵ (τ) obtained from the collisional Boltzmann equation, for spherical particles of a single radius, is shown in Fig. 3. It is determined by requiring

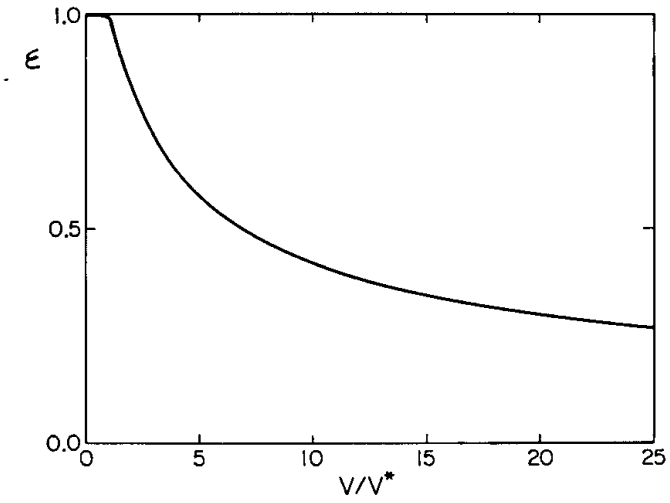

Fig. 2. The coefficient of restitution as a function of impact velocity.

that the rate at which energy is fed into random motions by the viscous stress balance the rate at which the energy of random motions is dissipated in inelastic collisions. The following gedanken experiment may help to clarify the point. Imagine setting up initial conditions such that every particle moves on a circular equatorial orbit. Collisions would occur as a consequence of differential rotation and the finite size of the particles. At first the impacts would be very gentle and almost perfectly elastic and the random velocity would grow. After a few collision times the radial distance traversed between collisions would be larger than the particle radius. The random velocity would begin to increase exponentially on the collision time scale and as it did so the impacts would become less elastic. Eventually the rate at which energy was being dissipated would balance the rate at which it was being converted into random motions by collisional stresses acting on the differential rotation. At this stage the random velocity would have reached equilibrium. The coefficient of restitution plotted in Fig. 3 is that which pertains to this equilibrium.

The monotonic increase of ϵ with increasing τ reflects the monotonic decrease of the radial distance traversed between collisions with increasing τ (at a fixed value of the random velocity). The latter implies that, per collision, the efficiency of conversion of orbital energy into the energy of random motions decreases with increasing optical depth. Thus, at equilibrium, the fraction of the relative kinetic energy dissipated per collision must be a monotonically decreasing function of τ.

We combine the ϵ (v) relation obtained from Andrews' theory with the ϵ (τ) relation described here to derive predictions for the random velocity v and the vertical thickness as functions of τ. The results are displayed in Fig. 4. They provide the theoretical justification for why Saturn's rings are so flat. We have neglected gravitational interactions between particles in the discussion of the random velocity. Pure gravitational scatterings act like physical

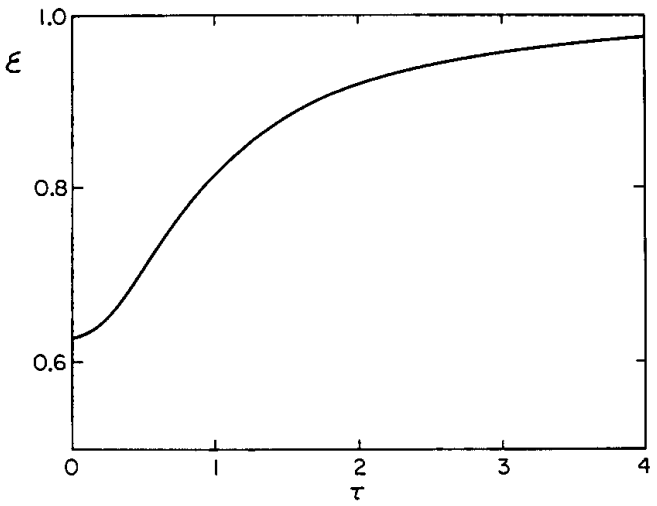

Fig. 3. The equilibrium value of the coefficient of restitution as a function of optical depth.

collisions with $\epsilon = 1$. Gravitational scatterings of small particles by large ones could significantly increase the random velocities of the small particles (Cuzzi et al. 1979).

B. Perturbed Disks

In regions of the rings where satellites exert torques, near sharp edges or resonances, the local rate of energy dissipation is enhanced. An argument we have given elsewhere (Borderies et al. 1982) shows that even in perturbed regions the shear cannot be much larger than the orbital angular velocity Ω unless $\tau >> 1$. Thus the viscosity, and consequently the velocity dispersion and ring thickness, must be enhanced in perturbed regions. In some places v and h may be increased above their unperturbed values by between one and two orders of magnitude.

III. PARTICLE SIZE

The distribution of particle size must depend upon the mechanical properties of the particles. The detailed physics which determines this distribution is not known.

A. Erosion Time Scale

Is the current size distribution the result of an equilibrium or of initial conditions? The particles are constantly being eroded by collisions and they accrete the resulting debris. The erosion time scale is the reciprocal of the product of the collision rate $\Omega\tau$ and the fractional mass lost per collision f. In a Keplerian disk the impact velocity is typically a few times v*, the minimum impact velocity at which fracture occurs. We estimate f to be of order $(a^*/R)^3$, where a^* is the radius of the contact area in an impact at relative velocity v*.

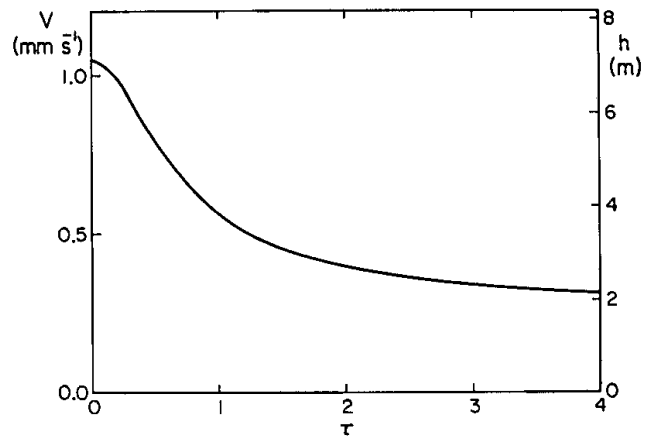

Fig. 4. The random velocity and disk thickness as a function of optical depth.

From Eqs. (1) and (4) and the values of E and σ_Y adopted in Sec. I, we obtain

$$t_{\text{erosion}} \simeq \frac{1}{\Omega\tau}\left(\frac{E}{\sigma_Y}\right)^3 \simeq \frac{10^5}{\tau}\ \text{yr}\,. \tag{5}$$

Since the estimated erosion time scale is much shorter than the age of the solar system we conclude that the particle size distribution results from an equilibrium between ongoing processes.

Three assumptions implicit in the derivation of the erosion time scale are worth mentioning: (1) we have assumed that a significant portion of the fractured material is lost from the particles; (2) we have neglected surface roughness which could affect the volume of fractured material; (3) we have assumed that v* given by Eq. (4) is a typical value for the impact velocity. This assumption is invalid if v* is smaller than ΩR. In this case the collision velocities would be of order ΩR. This qualification clarifies the seemingly unphysical conclusion that might otherwise be drawn from Eq. (5), namely, that the erosion time scale diverges as σ_Y approaches zero.

B. Range of Particle Sizes

If the processes responsible for establishing the particle size distribution did not single out any characteristic length scales, the distribution would be a power law. In fact, the differential number density per unit radius deduced from the Voyager radio occultation (Marouf et al. 1983) may be crudely fit by the power law

$$n(R) = K R^{-3.3} \tag{6}$$

for particle radii between a few centimeters and a few meters. The distribution

is cut off outside this range although precise details of the cutoffs, in particular the lower one, are lacking. The approximate power law is such that the larger particles contain most of the mass and the smaller ones provide most of the surface area. Independent information supports the existence of these two cutoffs. The observation that the optical depth is similar at visible and radio wavelengths proves that subcentimeter particles do not dominate the surface area. An upper cutoff is indicated because the radio determination of the surface mass density due to particles in the centimeter-to-meter-size range is, if anything, somewhat greater than that determined from the wavelengths of density and bending waves which provide a measure of the surface mass density from particles of all sizes. The radio determination of the surface mass density is based on the assumptions that the particles are made of solid ice and that the filling factor is low. In fact, the previous comparison suggests that one or both of these assumptions is invalid, a possibility to which we shall return later.

1. Upper Cutoff. Consider two critical orbital radii related to gravitational binding (see also chapter by Weidenschilling et al.). The inner r_1 is the limit inside which small particles are not gravitationally bound to a synchronously rotating, rigid sphere along the line passing from the center of the planet through the center of the sphere. The outer r_2 is the Roche limit within which no equilibrium exists for a synchronously rotating, incompressible, homogeneous fluid.

$$r_1/R_p = 1.44\,(\rho_p/\rho)^{\frac{1}{3}}, \tag{7}$$

$$r_2/R_p = 2.46\,(\rho_p/\rho)^{\frac{1}{3}}, \tag{8}$$

where ρ_p and ρ are the mean densities of the planet and the sphere and R_p is the planet's radius. The Roche limit r_2 is larger than r_1 because the quadrupole potential of a tidally deformed fluid enhances the disruptive effect of the tidal potential.

The two critical orbital radii are precisely defined but their application to planetary rings is fuzzy. A requirement for the persistence of a ring is that the particles do not form large satellites. Gravity is almost certainly the dominant force involved in satellite formation but it is difficult to see how to deduce a precise criterion for the location of the outermost possible boundary for a planetary ring.

The gravitational binding of small particles on the surface of a larger rigid body would be an appropriate criterion if the small particles eventually became chemically bound to the larger body. The large body would grow by devouring small particles and would remain rigid. On the other hand, if small

particles clustered gravitationally about a larger body and chemical bonding did not occur, the assemblage would have low shear strength and thus be mechanically similar to an incompressible, homogeneous, fluid body. Even if we could decide which of these scenarios described more closely the behavior of particles in Saturn's rings, we could not use r_1 or r_2 to make precise predictions because the bodies are not synchronously rotating.

It is of interest to compute the densities of particles for which r_1 or r_2 would coincide with the outer edge of Saturn's A Ring which is located at $2.26\,R_p$. We find $\rho \simeq 0.2$ g cm^{-3} and $\rho \simeq 0.8$ g cm^{-3}, respectively. It is plausible that the particles in Saturn's rings are less dense than solid ice for which $\rho \simeq 0.9$ g cm^{-3}; the Voyager radio occultation results offer some support for this view (Marouf et al. 1983). We conclude that permanent, gravitational binding of the ring particles does not generally occur, but that our understanding of the reason for this is incomplete (see chapter by Weidenschilling et al. for additional discussion of these issues).

Although gravity does not bind ring particles, molecular bonds can. The tidal stress in a particle of radius R is approximately $\sigma_t \simeq \rho\,(\Omega R)^2$. It is equal to the yield stress for $R = 10^3$ km. Obviously, this criterion is irrelevant to the upper cutoff on the size of particles in Saturn's rings.

A plausible argument can be made for identifying the vertical scale height of the rings with the upper cutoff. Suppose that the principal processes which determine the size distribution are collisional erosion and the accretion of the resulting debris. The accretion rate per unit area should be the same for all bodies smaller than the vertical scale height. The erosion of bodies will primarily be due to collisions with particles whose size is near the lower cutoff since they dominate the total area. The erosion rate per unit surface area should be similar for all bodies smaller than the vertical scale height. Typical impact velocities on these bodies are of order the random velocity. For particles large enough to stick out of the main particle layer, i.e. for those with $R > h$, due to differential rotation the typical impact velocity is of order ΩR which is larger than the random velocity. The ratio of the average erosion rate per unit area to the average accretion rate per unit area should be independent of size for $R < h$ and increase with R for $R > h$ since the volume of the material fractured during a collision must be an increasing function of the impact velocity; Andrews' theory predicts that it is proportional to the 3/2 power of v for v >> v*. It follows that if the net effect of erosion and accretion is to make $dR/dt = 0$ for bodies with $R < h$, then $dR/dt < 0$ for bodies with $R > h$ and the upper cutoff is naturally explained.

A problem with this picture is that the vertical thickness of the rings deduced from the damping lengths of density and bending waves appears to be somewhat larger than the upper cutoff, at least in the A Ring (Cuzzi et al. 1981; Lane et al. 1982; Lissauer et al. 1982; Shu et al. 1983). However, a smaller estimate is derived in Sec. V.B.5.

2. Lower Cutoff. The lower cutoff may be due to the sticking of small particles to bodies of comparable or larger size following collisions. To assess this possibility we compare the elastic energy W_E stored during an impact to the binding energy W_B which would be released if the material bonded across the contact area. The elastic energy is a significant fraction of the relative kinetic energy $M\mathrm{v}^2/2$. The surface binding energy is approximately $W_B \simeq Eia^2$, where $i \simeq 10^{-8}$ cm is the bond length and a is the radius of the contact area. We evaluate the ratio of these energies for $\mathrm{v} = \mathrm{v}^*$, since as we have seen, v is of order a few times v* in unperturbed regions of the rings. We obtain

$$\frac{W_B}{W_E} \simeq \frac{Eia^{*2}}{\rho R^3 \mathrm{v}^{*2}} \simeq \frac{i}{R}\left(\frac{E}{\sigma_Y}\right)^3 \simeq \frac{10\text{ cm}}{R}. \tag{9}$$

This result suggests that if molecular bonds form across the contact area particles smaller than a few centimeters may stick during collisions.

The sticking hypothesis needs to be critically examined; it is not obvious that molecular bonds form during low-velocity impacts and the fractures which occur in the contact region complicate the dynamics. Also, it is difficult to reconcile the sticking hypothesis with the observation that in certain portions of the rings micron size particles make a detectable contribution to the optical depth at visible wavelengths.

3. Thermal Stresses. Thermal stresses are produced as the particles spin and move in and out of Saturn's shadow. D. Stevenson (personal communication) has pointed out that thermal stresses may be responsible for a size-dependent erosion rate. These stresses are of order

$$\sigma_T \simeq \alpha \Delta T E, \tag{10}$$

where α is the coefficient of linear thermal expansion and ΔT is the temperature variation. The value $\alpha = 5 \times 10^{-6}\ \mathrm{K}^{-1}$ is appropriate for solid ice at the ring temperature (Hobbs 1974) and eclipse cooling measurements indicate that temperature variations of order 10 K penetrate to depths of several millimeters (Froidevaux and Ingersoll 1980; Froidevaux et al. 1981). Thus σ_T is of order 5×10^6 dyne cm^{-2} which, although smaller than the yield stress, is large enough to suggest that fractures may result from thermal stress.

It is probably at least as difficult to evaluate the erosion rate due to thermal stresses as that due to collisional stresses. The thermal and collisional time scales are of the same order of magnitude and the thermal and collisional stresses penetrate to comparable depths. Unlike the collisional stresses which are concentrated around the small area of contact, the thermal stresses are spread over a large fraction of the particle surface.

The spin angular velocity must decrease with increasing particle size as a consequence of the tendency of elastic collisions to promote equipartition of

kinetic energy, although due to the imperfectly elastic nature of the collisions equipartition is not achieved. The erosion rate per unit area due to thermal stresses should increase with particle size because the depth of penetration of the thermal wave is proportional to the square root of the spin period.

4. Commentary. Our discussion of the physical processes that determine the size distribution is far from conclusive. Even some of the assumptions made in deducing the distribution from the Voyager radio occultation data are open to question. It is crucial that the particles have shapes that are not too irregular and that they are well separated (Marouf et al. 1982, 1983). Otherwise, some of the scattering attributed to small particles may be due to surface roughness on larger bodies and the gravitational clustering of small particles, such as proposed to explain the azimuthal asymmetry of the A Ring (Colombo et al. 1976), could be partially responsible for the scattering attributed to the larger bodies.

The high abundance of micron-size particles in the F Ring and the outer A Ring suggests that small particles are collisionally produced since the random velocity is enhanced in those regions by satellite perturbations. The surface area of the micron size dust is so large that only a small fraction of it could be produced on the collisional time scale. Most likely the dust grains adhere weakly to the surfaces of larger particles and are shaken off in impacts. The high abundance of micron-sized particles in the B Ring, where perturbations due to external satellites are not especially significant, hints that an enhanced velocity dispersion may be maintained in that ring by small imbedded satellites. These satellites could be in part responsible for the qualitative morphological differences between the A and B Rings.

IV. LARGE-SCALE STRUCTURE OF RINGS

Collisions conserve angular momentum and dissipate energy. As a consequence of differential rotation, angular momentum is transferred outward and the ring spreads. The characteristic spreading time for a ring of radial width Δr is

$$t_{\text{spread}} \simeq (\Delta r)^2/\nu \ . \tag{11}$$

The kinematic viscosity ν is given by

$$\nu \simeq 0.5 \frac{v^2}{\Omega} \frac{\tau}{1+\tau^2} , \tag{12}$$

where v is the random velocity (Goldreich and Tremaine 1978*a*). We apply Eqs. (11) and (12) to estimate v in Saturn's rings by assuming that the rings have spread from a much narrower initial state to their present width over the

age of the solar system. This procedure yields $v \simeq 0.2$ cm s^{-1} which is between the theoretical estimate given in Sec. II and the value obtained from the damping lengths of density and bending waves.

The overall radial width of the rings could be explained by viscous diffusion but the great amount and variety of structure seen on all smaller scales implies that other mechanisms shape the detailed morphology. Among the outstanding features to explain are: the differences between the classical A, B and C Rings, the multiple ringlets which characterize the B Ring, the sharp outer edges of the A and B Rings and the clear gaps which often contain narrow elliptical ringlets. Two general mechanisms have been proposed to account for some of the structure seen in the rings. They are the viscous instability and satellite perturbations. We discuss them below.

A. Viscous Instability

The torque exerted by the ring material inside radius r on the material outside this radius is given by (Lynden-Bell and Pringle 1974)

$$T_v = 3\pi\nu\Sigma\Omega r^2 . \tag{13}$$

This torque is the rate at which angular momentum flows outward across the circle of radius r; it is also referred to as the viscous angular momentum luminosity L_H. The product $\nu\Sigma$ determines local structure since it is the only part of T_v which can vary on a scale small compared to r. We have computed $\nu\Sigma$ as a function of optical depth from the $v(\tau)$ relation shown in Fig. 4 and the expression for the kinematic viscosity given by Eq. (12). The result is displayed in Fig. 5. Note that this theoretical result, which predicts that $\nu\Sigma$ has a single maximum at $\tau = \tau_M \simeq 0.5$, is based on the assumption that the filling factor is small. For sufficiently large τ, the random velocity would be so low that this assumption would be invalid. We expect that a more complete theory would show that $\nu\Sigma$ increases for sufficiently large τ.

The viscous instability occurs in regions where $\nu\Sigma$ decreases with increasing τ, i.e. for $\tau > \tau_M$. The instability arises as follows (Lin and Bodenheimer 1981; Lukkari 1981; Ward 1981; chapter by Stewart et al.). The net viscous torque on a ringlet is proportional to $\partial(\nu\Sigma)/\partial r = \partial(\nu\Sigma)/\partial\tau \cdot \partial\tau/\partial r$. If $\partial(\nu\Sigma)/\partial\tau < 0$, ringlets move toward regions of enhanced optical depth and away from regions of reduced optical depth; thus a uniform disk with $\tau > \tau_M \simeq 0.5$ is unstable. The instability drives the disk toward a final state in which there are contiguous regions of high and low optical depth with identical values of T_v or $\nu\Sigma$.

The viscous instability is the leading contender for explaining the multi-ringlet structure of the B Ring. However, the current version of the theory predicts a bimodal optical depth distribution which is not observed. Also, it seems far-fetched to imagine that this instability could be responsible for the structure seen in regions of low average optical depth such as the C Ring and the Cassini Division.

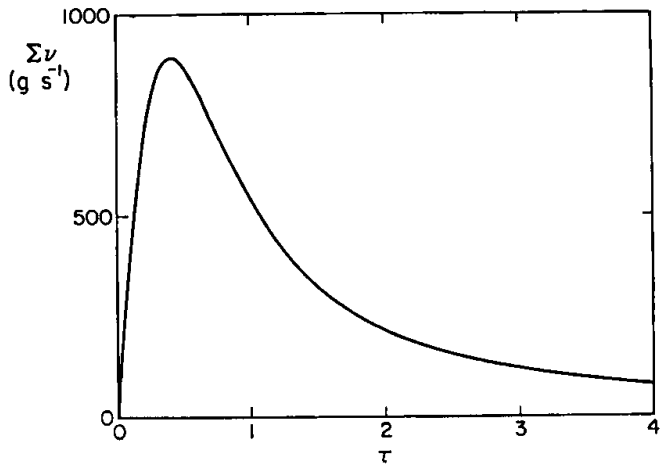

Fig. 5. The product $\nu\Sigma$ as a function of optical depth.

B. Satellite Perturbations

Satellites exert torques on the ring material in the neighborhood of resonances. The density and bending waves seen in Saturn's rings are due to torques produced by known satellites whose orbits are external to the main rings. Torques exerted by the shepherd satellites confine the F Ring. The sharp outer edge of the B Ring is maintained by the torque produced by Mimas at its 2:1 resonance and the sharp outer edge of the A Ring appears to be governed by the torque from the coorbital satellites at their 7:6 resonance. Torques produced by small satellites imbedded in the rings have been proposed to explain much of the small-scale structure. There is good circumstantial evidence that the Encke Division is kept open by small satellites that orbit within it (see chapter by Cuzzi et al.). However, in spite of a careful search, the satellites suspected of maintaining the inner and outer clear gaps in the Cassini Division were not detected by Voyager (Smith et al. 1982). Also, the absence of clear gaps in the B Ring has been taken as evidence that imbedded satellites are not responsible for its multi-ringlet structure (Lane et al. 1982). However, see the final paragraph in Sec. V.C for further discussion of this point.

V. SATELLITE TORQUES

Satellite torques are clearly associated with a variety of ring features. Nevertheless, we are far from having achieved a complete understanding of how they work. Some of the issues that remain to be settled are raised below. A bewildering variety of satellite torques is discussed in this section. To reduce confusion we adopt the following conventions: The satellite torques are exerted on rings and not on satellites. Both satellites and ring particles are

assumed to move on circular orbits. To simplify notation the satellite orbit is taken to be larger than the ring particle orbits. With these conventions, the satellite torques are negative. The discussion can be translated easily to the case where the satellite orbit is smaller than that of the ring particles. We use T to denote a torque; the superscripts L and NL indicate that the perturbation where the torque is applied is either linear or nonlinear; the critical torque which separates the linear and nonlinear torques is indicated by the superscript C; the subscripts m and s denote the torque at an isolated resonance of order m in a ring of uniform surface density and the total torque on a narrow ringlet. The satellite torques will be compared to the viscous torque which is given by Eq. (13).

A. Isolated and Overlapping Resonances

Two formulae for the satellite torque obtained from linear perturbation theory are available. They apply to isolated and overlapping resonances and read (Goldreich and Tremaine 1982)

$$T_m^L \simeq -f_1 m^2 \left(\frac{M_s}{M_p}\right)^2 \Sigma \Omega^2 r^4 , \tag{14}$$

$$T_s^L \simeq -f_2 \left(\frac{M_s}{M_p}\right)^2 \frac{\Sigma \Omega^2 r^7 \Delta r}{x^4} , \tag{15}$$

where M_s and M_p are the masses of the satellite and the planet. Equation (14) gives the torque at a Lindblad resonance which is located where

$$\Omega/\Omega_s = (r_s/r)^{\frac{3}{2}} = m/(m-1) . \tag{16}$$

Here Ω_s, Ω and r_s, r are the orbital angular velocities and orbital radii of the satellite and ring particle, m is a positive integer and f_1 is a numerical coefficient which is equal to 8.46 for $m >> 1$. Equation (15) gives the total torque on a narrow ringlet of width Δr which is separated from the satellite orbit by a distance $x = r_s - r << r$; $f_2 = 2.51$.

To relate the torque formulae given by Eqs. (14) and (15) we note that for $m >> 1$, the radial separation between neighboring Lindblad resonances is

$$d \simeq \frac{2r}{3m^2} . \tag{17}$$

It is straightforward to derive Eq. (15) from Eqs. (14) and (17). As long as there are several resonances within a narrow ringlet Eq. (15) gives the total satellite torque. It is the correct expression for the coarse grained satellite torque.

It is difficult to decide whether a resonance is truly isolated because the width is not a precise concept. Where we can neglect the collective effects due to self-gravity, it is natural to define the width as the radial distance over which the streamlines of the particle flow are significantly distorted. This definition yields $w \simeq (M_s/M_p)^{\frac{1}{2}} r$. Where self-gravity is important a density wave is launched at the resonance and its first wavelength provides a convenient measure for the resonance width. In this case $w = \{(8\pi^2 G\Sigma r)/[3\Omega^2(m-1)]\}^{\frac{1}{2}}$.

The resonances overlap if $d < w$. With either definition of w the A Ring resonances associated with the coorbital satellites and the shepherd satellites all qualify as isolated resonances and the shepherd satellite resonances in the F Ring overlap.

B. Linear and Nonlinear Satellite Torques

In the derivation of the standard formula for the torque at an isolated resonance, it is implicitly assumed that the ring has uniform surface density and that the disturbance is sufficiently weak so that linear perturbation theory is applicable. We examine these assumptions and the consequences of their violation below.

1. Linear and Nonlinear Density Waves. We consider linear waves first, and for the moment we neglect the effects of dissipation. The perturbation due to a satellite at an inner Lindblad resonance launches a trailing spiral density wave which propagates outward from the resonance. The density wave carries away from the resonance all of the negative angular momentum which the satellite torque adds to the disk. The ring particles undergo coherent oscillations in the wave. At the position of the resonance the oscillation frequency is equal to the epicyclic frequency and it falls steadily below the epicyclic frequency with increasing distance from the resonance. The lowering of the collective oscillation frequency below the epicyclic frequency is accomplished by the self-gravity of the disk material. The direction of propagation of the density wave is determined because self-gravity can lower but not raise the collective oscillation frequency. Since the necessary frequency tuning due to self-gravity increases with distance from the Lindblad resonance, the wavelength shortens in proportion to $(r-r_r)^{-1}$. As a consequence of the decreasing wavelength and the conservation of the angular momentum luminosity carried by the wave, the amplitude of the surface density perturbation increases in proportion to $r-r_r$. Thus, in the absence of damping all density waves would eventually become nonlinear.

We are primarily concerned with estimating the satellite torques at resonances and not with the propagation of density waves. We distinguish linear and nonlinear torques by the fractional surface density perturbation in the first wavelength of the density wave.

2. Linear Torques. For linear torques the important comparison is between the values of $|T_m{}^L|$ and T_v. If $|T_m{}^L| < T_v$, the surface density remains uniform in the vicinity of the resonance and the actual satellite torque is equal to $T_m{}^L$. On the other hand, if $|T_m{}^L| > T_v$, a gap is opened in the ring and the actual satellite torque is reduced to $-T_v$.

3. Nonlinear Torques. Nonlinear satellite torques are of great interest. All of the well-observed density waves in Saturn's rings are nonlinear in their first wavelengths. These include waves excited at the strongest resonances of the shepherd satellites, the coorbital satellites and Mimas.

The theory of nonlinear satellite torques has yet to be worked out. Most likely it will require numerical calculations. However, we can make an educated guess for the value of the torque by an appropriate extension of the linear theory. The basic assumption is that the nonlinear torque excites a density wave whose fractional surface density perturbation is of order unity. As such, the surface density perturbation is independent of the mass of the satellite. Since the satellite torque arises from the interaction between the satellite potential and the perturbed surface density, it must be proportional to the first power of the satellite mass. This is in contrast to the linear torque which is proportional to the second power of the satellite mass.

To obtain an explicit expression for the nonlinear satellite torque we use the linear theory to determine both the critical satellite mass and the critical torque for which the density wave is marginally nonlinear in its first wavelength. The nonlinear torque is obtained by multiplying the critical torque by the ratio of the actual satellite mass to the critical satellite mass. Expressions for the critical mass and the critical torque follow directly from results given in Goldreich and Tremaine (1978*b*). They are

$$M_s{}^C \simeq \frac{f_3 \Sigma r^2}{m}, \tag{18}$$

$$T_m{}^C \simeq \frac{-\pi^2 \Sigma^3 \Omega^2 r^8}{6 M_p{}^2}. \tag{19}$$

The nonlinear torque then reads

$$T_m{}^{NL} \simeq \frac{-f_4 m M_s \Sigma^2 \Omega^2 r^6}{M_p{}^2}. \tag{20}$$

For $m >> 1$, $f_3 = 0.44$ and $f_4 = 3.72$.

The density wave associated with a nonlinear satellite torque does not carry away from the resonance all of the angular momentum deposited in the disk. The limitation on its amplitude implies that its angular momentum

luminosity decays in proportion to $(r-r_r)^{-2}$ and that it is of order T_m^C within the first wavelength of the resonance. The nonlinear wave enhances the viscous stress which is responsible for its damping.

For nonlinear waves the important comparison is between $|T_m{}^{NL}|$ and T_ν. If $|T_m{}^{NL}| < T_\nu$, the actual satellite torque is equal to $T_m{}^{NL}$. On the other hand, if $|T_m{}^{NL}| > T_\nu$, a gap opens in the ring and the actual torque is reduced to $-T_\nu$.

4. Satellite Torque at a Sharp Edge. Sharp edges such as the outer edges of Saturn's A and B Rings are maintained by satellite torques. To maintain the edge the satellite torque must be equal to $-T_\nu$ evaluated in the unperturbed region interior to the edge. In the limit $M_s <$ (or $>$) $M_s{}^C = f_3 \Sigma\, r^2/m$, the maximum value of the satellite torque on a sharp edge is equal to T_m^L (or T_m^{NL}). The proof of this result follows directly from Eqs. (22)–(25) of Borderies et al. (1982).

5. Ring Viscosity. We apply the results of the preceding subsection to estimate the viscosity in Saturn's rings. The cleanest determination is obtained for the outer A Ring. The strongest resonances in this region are those due to the larger coorbital satellite (Lissauer and Cuzzi 1982). A nonlinear density wave but no gap is found at the position of the 6:5 resonance which implies that the viscous luminosity of angular momentum just inside the resonance exceeds the magnitude of the nonlinear satellite torque. The sharp outer edge coincides with the 7:6 resonance which tells us that the viscous luminosity of angular momentum just inside the edge is smaller than the magnitude of the nonlinear satellite torque. From these deductions and Eqs. (13) and (20) for T_ν and $T_m{}^{NL}$, we conclude that ν is $> 13(\Sigma/100\ \mathrm{g\ cm^{-2}})\ \mathrm{cm^2\ s^{-1}}$ just inside the 6:5 resonance and $< 16(\Sigma/100\ \mathrm{g\ cm^{-2}})\ \mathrm{cm^2\ s^{-1}}$ just inside the 7:6 resonance. To obtain the corresponding estimates for the velocity dispersion and ring thickness, we adopt $\Sigma = 50\ \mathrm{g\ cm^{-2}}$ and $\tau = 0.5$ for the outer A Ring and apply Eq. (12). We find $v = 0.07\ \mathrm{cm\ s^{-1}}$ and $h = 5$ m. These values are not very precise because they were derived using the expression for the nonlinear satellite torque which is itself an estimate.

C. Shepherding Torques

There has been considerable discussion of the confinement of narrow ringlets by pairs of small satellites (Goldreich and Tremaine 1979). Recent work has focused on the role of dissipation (Greenberg 1983). The standard explanation of the shepherding mechanism is as follows. Torques due to satellites tend to repel ring material. Therefore, narrow rings can be located between pairs of satellites where the net torque vanishes. The satellites exert a net positive torque on the inner half of the ring and a net negative torque on the outer half. These balance the viscous torque across the midline ring.

The explanation in the previous paragraph leads to a paradox which has thus far escaped attention. The satellites transfer energy as well as angular

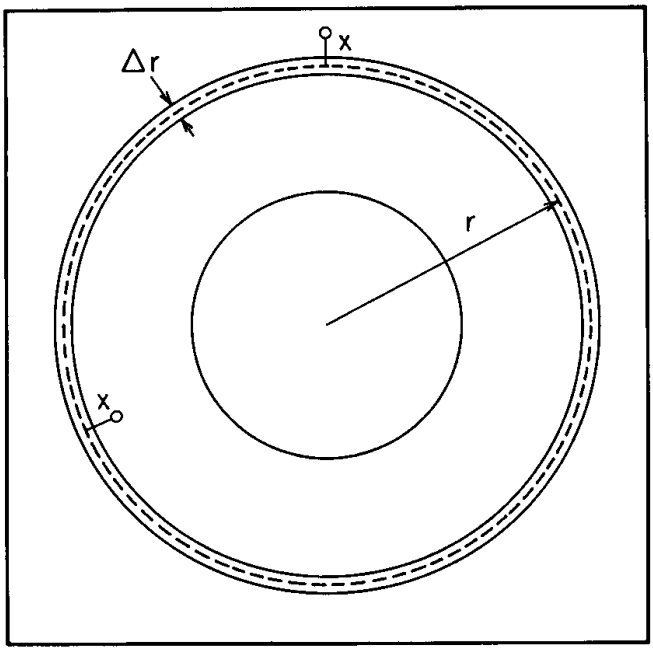

Fig. 6. Illustration of the shepherding geometry.

momentum to the ring. In a steady state the net torque vanishes but the net energy transfer is positive. The energy is dissipated by particle collisions. We now show that the viscous stress associated with the dissipation of energy appears to be so large that the satellites cannot confine the ring. Consider two identical satellites of mass M_s spaced a distance x from a narrow ringlet of width Δr (cf. Fig. 6). We assume that $\Delta r << x << r$. The ring and the satellite orbits are taken to be coplanar circles. We imagine the ring to be divided into an inner and an outer half. The total torques on the ring from the inner and outer shepherd satellites are denoted by $\mp T_s$. For our purpose we only need to know that the magnitude of T_s decreases with increasing x. It is irrelevant whether the torque is linear or nonlinear. For definiteness we take T_s to be proportional to x^{-q}; $q = 4$ for linear torques and $q = 3$ for nonlinear torques.

The standard treatment of the shepherding mechanism involves equating to zero the net torque on each half of the ring. This procedure yields

$$T_s \simeq \frac{-2x}{q\Delta r} T_{\nu} , \tag{21}$$

where T_{ν} is evaluated at the midline of the ring.

We extend the standard theory by relating T_s to the energy dissipated in the ring. For simplicity we assume that the ring is in a steady state. The Jacobi constant

$$J = E - \Omega_s \dot{H} \tag{22}$$

is conserved during an interaction with a satellite whose orbital angular velocity is Ω_s. Here E and H are the total energy and angular momentum of the ring. From this relation we deduce that the satellites transfer energy to the ring at a rate

$$\frac{dE}{dt} \simeq -3\frac{x}{r}\Omega T_s \,. \tag{23}$$

In a steady state this energy is dissipated in particle collisions so we have

$$\frac{dE}{dt} \simeq -M_r \frac{v^2}{t_c} \simeq -2\pi\, r\Delta r\, \Sigma v^2 \Omega\tau \,. \tag{24}$$

In writing Eq. (24) we have set the collision frequency equal to $\Omega\tau$ and assumed that a significant fraction of the relative kinetic energy of colliding particles is dissipated. Next we use Eqs. (12) and (13) to rewrite Eq. (24) as

$$\frac{dE}{dt} \simeq \frac{-4}{3}\,(1+\tau^2)\,\frac{\Delta r}{r}\,\Omega T_v \,. \tag{25}$$

Finally, we add the contributions to dE/dt given by Eqs. (23) and (25) which sum to zero to obtain

$$T_s \simeq \frac{-4}{9}\,(1+\tau^2)\,\frac{\Delta r}{x}\,T_v \,. \tag{26}$$

Comparison of Eqs. (21) and (26) reveals a contradiction with our beginning assumption that $\Delta r << x$. The origin of the problem is clear. The satellites produce torques that tend to confine the ring but they also transfer so much energy to it that confinement is impossible.

Can this paradox be resolved or must the shepherding mechanism be discarded? The answer lies in recognizing the weak link in the chain of arguments which led to the paradox, namely the step relating the rate of energy dissipation to the viscous luminosity of angular momentum. This step would be valid if the satellite perturbations were axisymmetric but they are not. We have shown elsewhere (Borderies et al. 1982, 1983) that in nonaxisymmetric regions, the magnitude and even the sign of the viscous angular momentum luminosity are not simply related to the rate of energy dissipation. We believe that the resolution of the shepherding paradox follows along these lines.

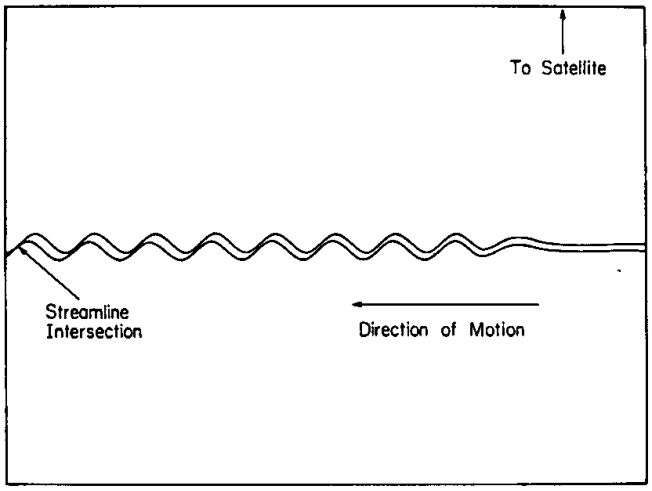

Fig. 7. Collision between neighboring streamlines following perturbation by a shepherding satellite. The horizontal scale is compressed relative to the vertical scale by a factor 75.

Some insight concerning the relation between energy dissipation and angular momentum transport in the shepherding process may be gained from Fig. 7. Shown there are two neighboring streamlines of initially circular test particle orbits perturbed by a shepherd satellite. Since the perturbed streamlines oscillate with slightly different wavelengths ($\lambda = 3\pi x$) they eventually intersect. The intersection occurs at quadrature, i.e., midway between periapse and apoapse. At the point of intersection the orbital angular velocity increases outward. Thus, if we were to assume that all of the energy dissipation and associated angular momentum transport occurred there, we would conclude that the angular momentum flowed inward, rather than outward as it does in unperturbed regions. The foregoing argument illustrates the subtlety of the relation between energy dissipation and angular momentum transport in perturbed regions. A more complete analysis indicates that the balance of the energy dissipation and angular momentum transport occurs well before the hypothetical streamline crossing for $\tau << 1$ and close to it for $\tau >> 1$.

Our assessment of this paradox suggests to us that the accepted description of the shepherding mechanism is seriously flawed. The old picture is correct in so far that the narrow rings are located between pairs of satellites where the net torque vanishes. However, the satellite torques are not responsible for confining the ring material. The confinement is due to the inward transport of angular momentum which accompanies the dissipation of the energy associated with the disturbances created in the ring by the shepherd satellites. This new view removes the problem of understanding the sharp

edges of the narrow rings. Also, although less obvious, the minimum sizes predicted for the satellites inferred to shepherd rings are diminished by a factor $\Delta r/x$.

A speculative possibility is that there are regions in Saturn's rings where the optical depth is so high that small imbedded satellites might be unable to clear gaps although they could still produce optical depth variations. Perhaps small satellites may still prove to be the cause of structure in the B Ring.

VI. TIME SCALE FOR SATELLITE ORBIT EVOLUTION

As external satellites extract angular momentum from the rings their orbits expand. Calculations based on the formula for the linear satellite torque predict remarkably short time scales for the recession of close satellites from the rings (Goldreich and Tremaine 1982). Accounting for the effects of nonlinearity lengthens the estimated time scales, perhaps by as much as an order of magnitude for 1980S27 and the coorbital satellites, less for 1980S26 and not at all for 1980S28. Thus these short time scales remain perhaps the most intriguing puzzle in planetary ring dynamics.

Since angular momentum may be transferred outward in resonant interactions between satellites (Goldreich 1965; Peale 1976), it is natural to inquire whether the inner satellites in question are involved in any orbital resonances with the more massive outer satellites. If they were, the time scale problem would be alleviated because the angular momentum taken from the rings by the inner satellites would largely go into expanding the orbits of these more massive bodies. We have spent considerable effort fruitlessly searching for appropriate two- and three-body resonances. We identified several close misses and a number of excellent candidates for past or future resonances but failed to find a single active resonance.

The severe nature of the problem is well-illustrated by the system composed of the F Ring and its two shepherd satellites, 1980S26 and 1980S27, hereafter called S26 and S27. Taken by themselves, S26 and S27 could have moved from the outer boundary of the A Ring to their present locations in approximately 2×10^7 yr and 4×10^6 yr, respectively. (These values are based on an assumed $\Sigma = 50$ g cm^{-2}.) The actual situation is more complicated. S27 is trapped between the A Ring and the F Ring and some of the angular momentum it takes from the A Ring is transferred outward to the F Ring. S26 takes angular momentum from the F Ring as well as from the A Ring. Since S27 is located closer to the A Ring and is more massive than S26, and presumably the F Ring as well, in the absence of interactions with additional bodies, the entire system would recede from the A Ring at the rate determined for S27 alone.

The outward movement of the system could be reduced if S26 were involved in a resonance with a more massive outer satellite. When the early results of the orbit determination of S26 showed that its mean motion was

close to 3/2 that of Mimas, everything seemed to be falling in place. S26 would transfer angular momentum to Mimas which would then pass most of it along to the more massive Tethys with which it is involved in a resonance. Hope for this solution died when a more accurate orbit determination demonstrated that the suspected resonance between S26 and Mimas was just a close miss.

No resonance has been found linking S26 with one or more outer satellites. What might this imply? Are the F Ring and its shepherd satellites very young? Does the long sought resonance exist awaiting detection? A most interesting possibility is that S26 is transferring angular momentum to Mimas even though the two bodies are not in an exact orbital resonance. This could be accomplished if the motion of S26 were chaotic, i.e., if the value of its mean motion were undergoing a slow random walk. We have proven that if the mean longitude of S26 were subject to a significant random drift, in addition to its dominant secular increase, angular momentum transfer to Mimas would take place by virtue of the near resonance between S26 and Mimas. By significant drift we mean of order one radian on the circulation time scale of the critical argument associated with the near resonance. To check this hypothesis, we must first determine whether the orbital motion of S26 is chaotic. To do so we need to investigate the perturbations of its orbit produced by S27. Solution of this and the other outstanding theoretical problems will await results of ongoing research.

Acknowledgments. N. B. acknowledges support from the National Science Foundation, US-France Exchange Postdoctoral Fellowship and Grant ATP Planétologie. P. G. and S. T. each acknowledge support from both the National Science Foundation and the National Aeronautics and Space Administration.

REFERENCES

Andrews, J. P. 1930. Theory of collision of spheres of soft metal. *Phil. Mag.* 9:593–610.

Borderies, N., Goldreich, P., and Tremaine, S. 1982. Sharp edges of planetary rings. *Nature* 299:209–211.

Borderies, N., Goldreich, P., and Tremaine, S. 1983. Perturbed particle disks. *Icarus* 55:124–132.

Colombo, G., Goldreich, P., and Harris, A. W. 1976. Spiral structure as an explanation for the asymmetric brightness of Saturn's A ring. *Nature* 264:344–345.

Cuzzi, J. N., Durisen, R. H., Burns, J. A., and Hamill, P. 1979. The vertical structure and thickness of Saturn's rings. *Icarus* 38:54–68.

Cuzzi, J. N., Lissauer, J. J., and Shu, F. H. 1981. Density waves in Saturn's rings. *Nature* 292:703–707.

Froidevaux, L., and Ingersoll, A. P. 1980. Temperatures and optical depths of Saturn's rings and a brightness temperature from Titan. *J. Geophys. Res.* 85:5929–5936.

Froidevaux, L., Matthews, K., and Neugebauer, G. 1981. Thermal response of Saturn's ring particles during and after eclipse. *Icarus* 46:18–26.

Goldreich, P. 1965. An explanation of the frequent occurrence of commensurable mean motions in the solar system. *Mon. Not. Roy. Astron. Soc.* 130:159–181.

Goldreich, P., and Tremaine, S. 1978*a*. The velocity dispersion in Saturn's rings. *Icarus* 34:227–239.

Goldreich, P., and Tremaine, S. 1978*b*. The formation of the Cassini Division in Saturn's rings. *Icarus* 34:240–253.

Goldreich, P., and Tremaine, S. 1979. Towards a theory for the Uranian rings. *Nature* 277:97–99.

Goldreich, P., and Tremaine, S. 1982. The dynamics of planetary rings. *Ann. Rev. Astron. Astrophys.* 20:249–283.

Greenberg, R. 1983. The role of dissipation in shepherding of ring particles. *Icarus* 53: 207–218.

Hertz, H. 1881. Uber die beruhrung fester elastischer kozper. *J. Reine Angew. Math. (Crelle)* 92:156–171.

Hobbs, P. V. 1974. *Ice Physics* (London: Oxford Univ. Press, Clarendon).

Lane, A. L., Hord, C. W., West, R. A., Esposito, L. W., Coffeen, D. L., Sato, M., Simmons, K. E., Pomphrey, R. B., and Morris, R. B. 1982. Photopolarimetry from Voyager 2: Preliminary results on Saturn, Titan and the rings. *Science* 215:537–543.

Lin, D. N. C., and Bodenheimer, P. 1981. On the stability of Saturn's rings. *Astrophys. J. Lett.* 248:L83–L86.

Lissauer, J. J. and Cuzzi, J. N. 1982. Resonances in Saturn's rings. *Astron. J.* 87:1051–1058.

Lissauer, J. J., Shu, F. H., and Cuzzi, J. N. 1982. Viscosity in Saturn rings. Proceedings of *I.A.U. Colloquium 75. Planetary Rings,* ed. A. Brahic, Toulouse, France, Aug. 1982.

Lukkari, J. 1981. Collisional amplification of density fluctuations in Saturn's rings. *Nature* 292:433–435.

Lynden-Bell, D., and Pringle, J. 1974. The evolution of viscous disks and the origin of the nebular variables. *Mon. Not. Roy. Astron. Soc.* 168:603–637.

Marouf, E. A., Tyler, G. L., and Eshleman, V. R. 1982. Theory of radio occultation by Saturn's rings. *Icarus* 49:161–193.

Marouf, E. A., Tyler, G. L., Zebker, H. A., Simpson, R. A., and Eshleman, V. R. 1983. Particle-size distributions in Saturn's rings from Voyager 1 radio-occultation. *Icarus* 54: 189–211.

Parameswaran, V. R., and Jones, S. J. 1975. Brittle fracture of ice at 77 K. *J. Glaciology* 14:305–315.

Peale, S. J. 1976. Orbital resonances in the solar system. *Ann. Rev. Astron. Astrophys.* 14:215–246.

Shu, F. H., Cuzzi, J. N., and Lissauer, J. J. 1983. Bending waves in Saturn's rings. *Icarus* 53:185–206.

Smith, B. A., Soderblom, L., Batson, R., Bridges, P., Inge, J., Masursky, H., Shoemaker, E., Beebe, R., Boyce, J., Briggs, G., Bunker, A., Collins, S. A., Hansen, C. J., Johnson, T. V., Mitchell, J. L., Terrile, R. J., Cook II, A. F., Cuzzi, J., Pollack, J. B., Danielson, G. E., Ingersoll, A. P., Davies, M. E., Hunt, G. E., Morrison, D., Owen, T., Sagan, C., Veverka, J., Strom, R., and Suomi, V. E. 1982. A new look at the Saturn system: The Voyager 2 images. *Science* 215:504–537.

Ward, W. R. 1981. On the radial structure of Saturn's rings. *Geophys. Res. Letters* 8:641–643.